Journal Pre-proof

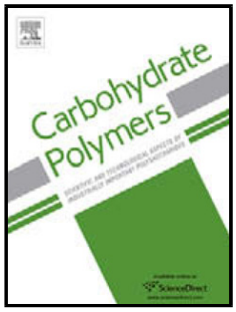

Magnetic chitosan-copper nanocomposite: A plant assembled catalyst for the synthesis of amino- and *N*-sulfonyl tetrazoles in eco-friendly media

Narjes Motahharifar, Mahmoud Nasrollahzadeh, Asghar Taheri-Kafrani, Rajender S. Varma, Mohammadreza Shokouhimehr

PII: S0144-8617(19)31487-0

DOI: https://doi.org/10.1016/j.carbpol.2019.115819

Reference: CARP 115819

To appear in: *Carbohydrate Polymers*

Received Date: 7 October 2019

Revised Date: 25 December 2019

Accepted Date: 30 December 2019

Please cite this article as: Motahharifar N, Nasrollahzadeh M, Taheri-Kafrani A, Varma RS, Shokouhimehr M, Magnetic chitosan-copper nanocomposite: A plant assembled catalyst for the synthesis of amino- and *N*-sulfonyl tetrazoles in eco-friendly media, *Carbohydrate Polymers* (2019), doi: https://doi.org/10.1016/j.carbpol.2019.115819

Magnetic chitosan-copper nanocomposite: A plant assembled catalyst for the synthesis of amino- and *N*-sulfonyl tetrazoles in eco-friendly media

Narjes Motahharifar,[a] Mahmoud Nasrollahzadeh[a,*] Asghar Taheri-Kafrani[b,] Rajender S. Varma[c] and Mohammadreza Shokouhimehr[d,*]

[a]*Department of Chemistry, Faculty of Science, University of Qom, Qom 3716146611, Iran*

[b]*Department of Biotechnology, Faculty of Advanced Sciences and Technologies, University of Isfahan, Isfahan 81746-73441, Iran*

[c]*Regional Centre of Advanced Technologies and Materials, Department of Physical Chemistry, Faculty of Science, Palacky University, Šlechtitelů 27, 783 71 Olomouc, Czech Republic*

[d]*Department of Materials Science and Engineering, Research Institute of Advanced Materials, Seoul National University, Seoul 08826, Republic of Korea*

*Corresponding authors e-mail addresses: mahmoudnasr81@gmail.com (M. Nasrollahzadeh), and mrsh2@snu.ac.kr (M. Shokouhimehr).

Graphical abstract

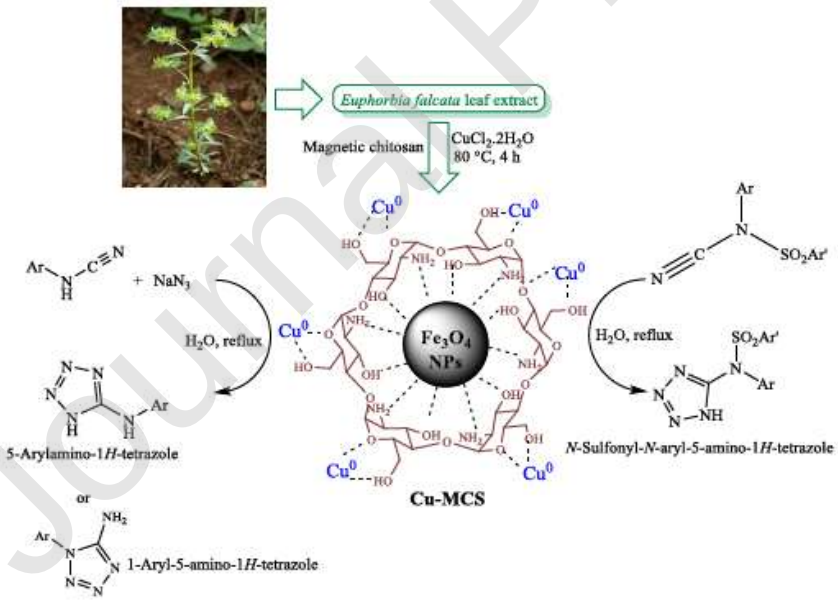

Highlights

- Synthesis of the magnetic chitosan-copper nanocomposite, Cu NPs@Fe_3O_4-chitosan.
- Cu NPs@Fe_3O_4-chitosan was characterized by FT-IR, XRD, TG/DTG, FESEM, TEM, HRTEM, VSM, elemental mapping and EDS.
- Synthesis of amino- and *N*-sulfonyl tetrazoles in eco-friendly media using Cu NPs@Fe_3O_4-chitosan.
- The catalyst can be easily recycled and reused five times without much loss in its catalytic efficiency.

ABSTRACT

A greener, cost efficient and simple method is described to prepare copper nanoparticles (NPs) immobilized on the magnetic chitosan (one of the more versatile polysaccharides) using *Euphorbia falcata* leaf extract as reducing/stabilizing agent. The prepared catalyst (Cu NPs@Fe_3O_4-chitosan) was authenticated by field emission scanning electron microscope (FESEM), X-ray diffraction (XRD), transmission electron microscopy (TEM), Scanning transmission electron microscopy (STEM), energy-dispersive X-ray spectroscopy (EDS), thermogravimetry/derivative thermogravimetry (TG/DTG), Vibrating sample magnetometer (VSM), and elemental mapping. TEM analysis indicates that Cu NPs with average sizes in 5-10 nm range is formed on magnetic chitosan with the spherical morphology. The Cu NPs@Fe_3O_4-chitosan was employed as a new catalyst for the synthesis of different tetrazoles by the reaction of various secondary or tertiary cyanamides with sodium azide in water under reflux conditions. Easy separation by external magnetic field, mild reaction conditions, low cost and the reusability are some of the beneficial features of this catalyst.

Keywords: Magnetic chitosan; Polysaccharide; Cu NPs@Fe_3O_4-chitosan; Nanocatalyst; Tetrazoles; Eco-friendly

1. Introduction

Tetrazoles are a versatile member of five-membered nitrogen heterocycles with unique properties such as highest acidity and number of N atoms, high formation enthalpy and lowest basicity with good stability. Among the azole heterocycles, tetrazoles manifest extensive abilities in diverse research areas as it has been applied in the medicinal chemistry as lipophilic spacers, material science as analytical reagents, propellants, and particularly as ligands for the

preparation of complexes (Frija, Cristiano, Gómez-Zavaglia, Reva, & Fausto, 2014; Frija, Ismael, & Cristiano, 2010; Ichinari, Nagaki, & Yoshida, 2017; Koldobskii, 2006; Nasrollahzadeh, Sajjadi, & Khonakdar, 2018; Ostrovskii, Popova, & Trifonov, 2017; Pino-Gonzalez, Romero-Carrasco, Calvo-Losada, Oña-Bernal, Quirante, & Sarabia, 2017; Wei, Bian, & Gong, 2015). Besides that, tetrazole derivatives have been effectively utilized as starting materials for synthesis of *N*-containing compounds (Burger, 1991; Frija, Ismael, & Cristiano, 2010; Gutmann, Glasnov, Razzaq, Goessler, Roberge, & Kappe, 2011). The importance of tetrazole-containing compounds as effective antitumor agents, antihypertensive drugs, and peptidase inhibitor has been also highlighted in the documented literature (Arshad, Bhat, Pokharel, Kim, Lee, Athar, & Choi, 2014; ElMonaem, Abdel-Aziz, Morsy, Badria, ElSenduny, El-Ashmawy, & Moustafa, 2016; Sajjadi, Nasrollahzadeh, & Sajadi, 2017; Schmidt, & Schieffer, 2003; Tanaka, Okuda, Yamamoto, 2004; Wexler, Greenlee, Irvin, Goldberg, Prendergast, Smith, & Timmermans, 1996).

Owing to widespread application, the research on their catalytic synthesis has been of huge interest, and particularly, arylaminotetrazoles have been a hot topic of fundamental investigation in view of their pharmaceutical and biological applications (Henry, Finnegan, & Lieber, 1954; Herr, 2002; Katritzky, Rees, & Scriven, 1996; Peet, Baugh, Sundler, Lewis, Matthews, Olberding, & Shah, 1986; Singh, Chawla, Kapoor, Paul, & Malhotra, 1980). The replacement of N atom affords *N*-substituted arylaminotetrazoles such as *N*-alkyl-, *N*-acyl-, and *N*-sulfonyl-arylaminotetrazoles and based on their unique structures, properties and applications, their synthesis should receive immense attentions, but for the lack of tenable procedures and inadequate synthetic methods (Miller, Feeney, Ma, Zarcone, Aziz, & Magnuson, 1990; Nasrollahzadeh, Sajjadi, Komber, Khonakdar, & Sajadi, 2019).

Traditional synthetic procedures have been reported for synthesis of aminotetrazole which entail (i) the condensation of carbodiimides, cyanamides, imidoyl chlorides, aminoiminomethanesulfonic acids, and/or thioureas with sodium azide (NaN_3), (ii) reaction of aminoguanidine with sodium nitrite ($NaNO_2$), (iii) reaction of tetrazoles-comprising a leaving group in 5-position with suitable amines, (iv) conversion of 1-aryltetrazoles to 1-arylaminotetrazoles via an one step consecutive ring-opening procedure by using NaN_3 and organolithium reagents under harsh conditions at -70 °C, (v) the reaction of cyanamide derivatives with hydrazoic acid (HN_3), and (vi) 1-substituted tetrazoles isomerization in the melt state or boiling ethylene glycol (Scheme 1) (Congreve, 1996; Garbrecht, & Herbst, 1953; Habibi, Nasrollahzadeh, Faraji, & Bayat, 2010; Henry, Finnegan, & Lieber, 1955; Sajjadi, Nasrollahzadeh, & Sajadi, 2017; Nasrollahzadeh, Habibi, Shahkarami, & Bayat, 2009; Vorobiey, Gaponik, Petrov, & Ivashkevich, 2006). Among the published protocols, most of them have several disadvantages *e.g*. the use of highly

toxic azide source, expensive/toxic reagents, high boiling solvents (*N*,*N*-dimethylformamide), homogeneous catalysts, tedious work-up, lower yields, harsh reaction conditions, and also formation of a mixture of isomers that restrict their applications.

Although arylaminotetrazoles have been recently accessed via [2 + 3] cycloaddition of monosubstituted cyanamides with NaN_3 using various catalysts like zeolite (Nasrollahzadeh, Habibi, Shahkarami, & Bayat, 2009), $ZnCl_2$ (Habibi, Nasrollahzadeh, Faraji, & Bayat, 2010), HOAc (Modarresi-Alam & Nasrollahzadeh, 2009), $FeCl_3$-SiO_2 (Habibi, & Nasrollahzadeh, 2010), Ag/Fe_3O_4 (Sajjadi, Nasrollahzadeh, & Sajadi, 2017) and Cu(II) complex (Nasrollahzadeh, Sajjadi, & Khonakdar, 2018), thus far, there is no report for the synthesis of *N*-sulfonyl tetrazoles. Hence, the advancement of straightforward approaches and eco-friendly catalytic procedures for the *N*-substituted tetrazoles is warranted to circumvent the abovementioned drawbacks and limitations.

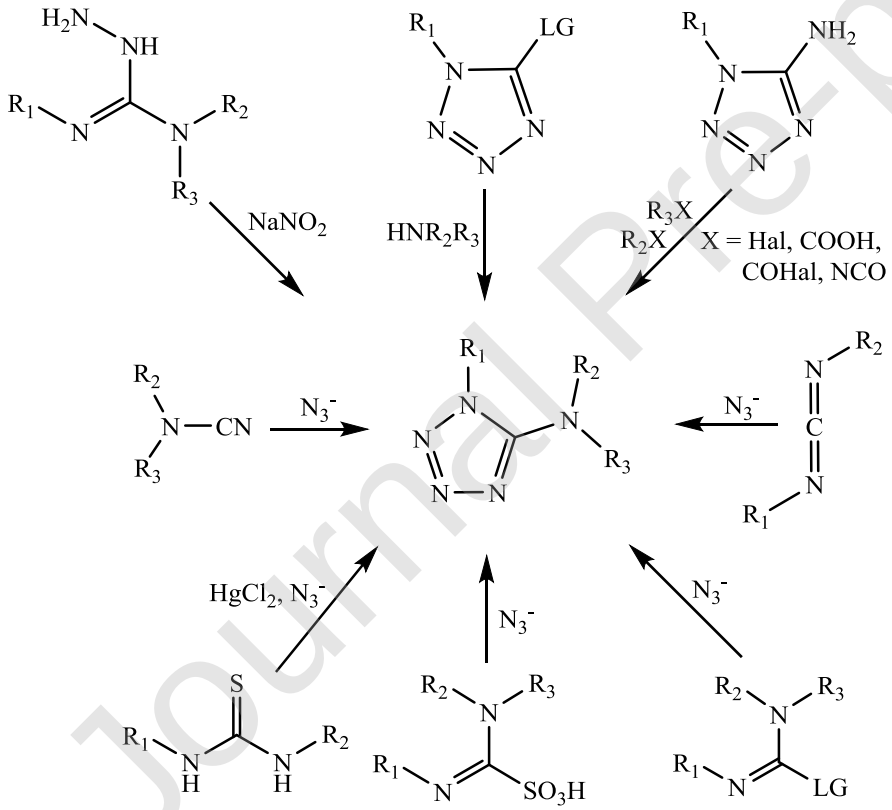

Scheme 1. Synthesis of aminotetrazoles using different methods.

Additionally, homogeneous catalytic systems (Yella, Khatun, Rout, & Patel, 2011) in various processes need to be substituted with heterogeneous systems due to inherent advantages of their recoverability, reusability, regenerability, and ease of handling (Baig, Nadagouda, & Varma, 2014; Li, & Guan, 2017; Nasrollahzadeh, Sajjadi, Komber,

Khonakdar, & Sajadi, 2019; Polshettiwar, & Varma, 2009; Rathi, Gawande, Pechousek, Tucek, Aparicio, Petr, & Zboril, 2016; Wang, Li, Zhang, O'Connor, Varma, Yu, & Hou, 2018). Over the decades, metal/metal oxide NPs like Pd, Ag, Au, Cu, Fe_3O_4, and TiO_2 have been investigated (Gawande, Branco, Varma, 2013; Hu, Liu, Wang, Liu, Liu, Jing, & Zhang, 2013; Nasrollahzadeh, Sajjadi, & Khonakdar, 2018; Oi, Choo, Lee, Ong, Hamid, & Juan, 2016; Sharma, Dutta, Sharma, Zboril, Varma, & Gawande, 2016; Titirici, White, Brun, Budarin, Su, del Monte, & MacLachlan, 2015; Varma, 2016; Xu & Wang, 2012), but the clustering of various NPs is generally inescapable. Due to environmental and economic significance, the catalysts heterogenization on the novel supports has been investigated especially magnetic NPs on polymer materials have garnered maximum attention as proficient nanocatalysts because of their propitious properties *e.g*. high surface energy, thermal stability, small size, high catalytic activity, and high magnetic permeability, among others (Hu, Liu, Wang, Liu, Liu, Jing, & Zhang, 2013; Nasrollahzadeh, Sajjadi, & Khonakdar, 2018; Nasrollahzadeh, Sajjadi, Komber, Khonakdar, & Sajadi, 2019; Sharma, Dutta, Sharma, Zboril, Varma, & Gawande, 2016).

The selection of renewable biopolymers such as alginate, egg-shell membrane, cellulose, starch, chitin, and especially chitosan (CS) comprise a pivotal aspect in the promotion of biodegradable catalysts. CS is one of the distinctive and most versatile biopolymers encompassing linear polysaccharides with reactive amino groups (*N*-deacetylated chitin), with relatively biocompatible, and inexpensive abundance compared to other biopolymers (Krajewska, 2004; Lee, Chen, & Den, 2015). The fusion of biopolymers and magnetic NPs can afford fascinating nanomagnetic support for easy recovery of nanocatalysts; the surface functionalities of CS are easily accessible for immobilization of metal/metal oxide NPs.

Several physicochemical approaches have been used for the synthesis of metal NPs but mostly suffer from limitations that present potential environmental risks which has prompted search for alternative eco-friendly and sustainable procedures. Nowadays, a variety of greener resources have been deployed to fabricate NPs which avoid the use of toxic reagents and organic solvents, harmful stabilizers and/or capping agents, longer reaction times, and high temperature calcinations (Banerjee, Satapathy, Mukhopahayay, & Das, 2004; Kou & Varma, 2012; Nadagouda & Varma, 2008; Nasrollahzadeh, Sajjadi, & Khonakdar, 2018; Nasrollahzadeh, Sajjadi, Komber, Khonakdar, & Sajadi, 2019; Plachtová, Medříková, Zbořil, Tuček, Varma, & Maršálek, 2018; Varma, 2012; Varma, 2014). Among these biological methods, the processes based on plant extracts or gums have been described in literature (Banerjee, Satapathy, Mukhopahayay, & Das, 2004; Kou & Varma, 2012; Nadagouda & Varma, 2008; Narayanan & Sakthivel,

2011; Plachtová, Medříková, Zbořil, Tuček, Varma, & Maršálek, 2018), the main benefits being an easy reaction system operating under soft conditions, application of safe solvents like water, absence of noxious and hazardous materials as well as compatibility for pharmaceutical and biomedical utilization (Abdel-Halim, El-Rafie, & Al-Deyab, 2011; Qazi, Hussain & Tahir, 2016).

The genus *Euphorbia* (spurge family) comprise several species as herbs, shrubs and trees with a wide distribution in the world; *Euphorbiaceae* family plants contain latex with unique flower structures (Citoğlu & Özbilgin, 2012; Irshad, Rubina, Wahib, Rukhsana, & Choudhary, 2009; Noori, Chehreghani, & Kaveh, 2009; El Bribri, Tabyaoui, Tabyaoui, El Attari, & Bentiss, 2013).

Herein, we report the production of 1-aryl-5-amino-1*H*-tetrazoles (**B** isomer), 5-arylamino-1*H*-tetrazoles (**A** isomer) and *N*- sulfonyl- *N*- aryl- 5- amino- 1*H*- tetrazoles *via* the reaction of secondary or tertiary cyanamides with NaN_3 in refluxed water using Cu NPs@Fe_3O_4-chitosan as a recyclable magnetic nanocatalyst with extraordinary catalytic prowess (Scheme 2) without the use of toxic reagents such as HN_3. The Cu NPs@Fe_3O_4-chitosan was formed via decoration of Cu NPs onto Fe_3O_4-chitosan nanostructure by *Euphorbia falcate* extract as a reducing and stabilizing agent. Green chemistry is reflected in the entire process of synthesis. 1-Aryl-5-amino-1*H*-tetrazoles (**B** isomer) and 5-arylamino-1*H*-tetrazoles (**A** isomer) were prepared in DMF in our research group, previously (Nasrollahzadeh, Habibi, Shahkarami, & Bayat, 2009). In the present work, tetrazoles were prepared in water as a green solvent. Water is cheap, non-combustible, non-toxic, non-explosive, and environmentally acceptable. The use of water as a solvent has several advantages, including avoiding the use of hazardous substances, preventing the generation of waste and minimization of energy requirements. The water-insolubility of tetrazoles further facilitates their isolation. Results show that the Cu NPs loaded on Fe_3O_4-chitosan exhibit excellent catalytic activity and good stability. On the other hand, to the best of our knowledge, this is the first report for the synthesis of *N*- sulfonyl- *N*- aryl- 5- amino- 1*H*- tetrazoles.

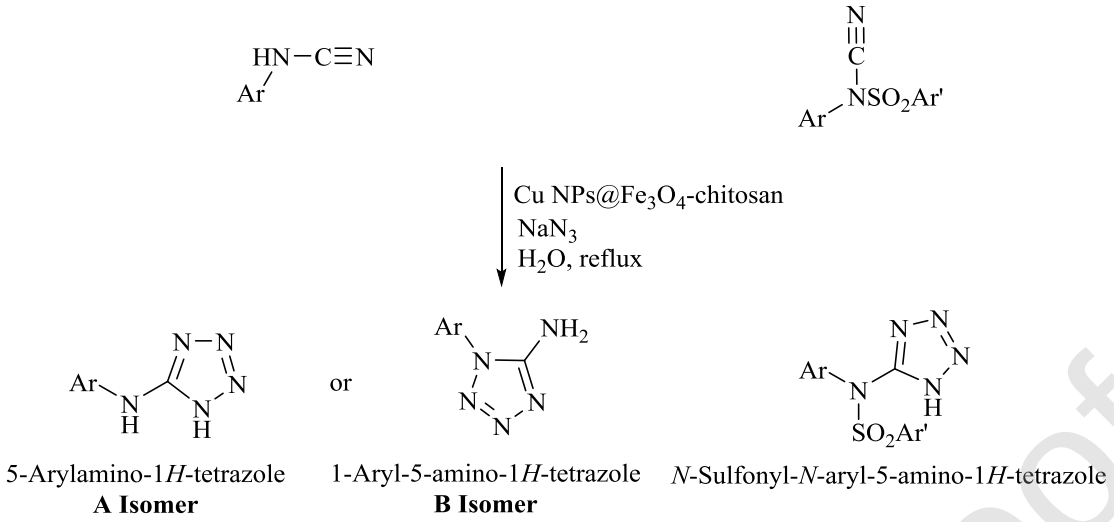

5-Arylamino-1*H*-tetrazole **A Isomer** | 1-Aryl-5-amino-1*H*-tetrazole **B Isomer** | *N*-Sulfonyl-*N*-aryl-5-amino-1*H*-tetrazole

Scheme 2. Synthesis of arylaminotetrazoles and *N*-sulfonyl-*N*-aryl-5-amino-1*H*-tetrazoles using Cu NPs@Fe_3O_4-chitosan nanocatalyst.

2. Experimental section

2.1 Instruments and reagents

All materials were procured from the Merck/Aldrich chemical company. Chitosan (De-acetylation degree: 85%, molecular weight: 50000-80000 Da (medium), particle dimension: powder with mesh size of 80, dissolvable in acetic acid 1%) was purchased from Nano Novin Polymer (NNP) Co., prepared by Shrimp shell waste. The structure of the products was confirmed by FT-IR, ^{1}HNMR, ^{13}CNMR, XRD, UV-visible, TEM, FESEM, EDS, and VSM. FT-IR, UV-Vis and NMR spectra were conducted by Perkin-Elmer 781, Hitachi-U-2900 and Bruker spectrometer Avance DRX-400 and 600 MHz, respectively. The Cu NPs@Fe_3O_4-chitosan size and morphology were characterized applying a TEM, JEM-F200 JEOL and FESEM, Hitachi S-4700. Next analysis, VSM and XRD measurements that were validated by Lake shore VSM-7410 magnetometer at 298 K and Philips PW 1373 diffractometer, respectively. The Cu NPs@Fe_3O_4-chitosan chemical composition was analyzed by EDS equipped in FESEM. TG/DTG analysis was performed by STA 1500 Rheometric-Scientific.

2.2 Preparation of extract of Euphorbia falcata

To achieve a suitable concentration of antioxidant phenolics (e.g; flavonoids) as highly soluble compounds in water, 50 g of dried plant in 300 mL double distilled water was heated for 0.5 h at 70 ºC. Then after cooling to room

temperature, the produced extract was centrifuged at 7000 rpm, then filtered and filtrate was kept in the refrigerator for the synthesis of Cu NPs.

2.3 Synthesis of Cu NPs

10 mL of 5 M $CuCl_2 \cdot 2H_2O$ solution was combined with 100 mL of aqueous extract at 70 °C. After 7 min, the mixture color was changed to dark due to Cu NPs formation. Then, the biosynthesized nanoparticles were separated via centrifugation at 7000 rpm for 30 min. Finally, the obtained precipitation washed with absolute alcohol to remove possible impurities.

2.4 Preparation of magnetic chitosan (MCS)

Fe_3O_4 NPs were prepared according to the literature by using co-precipitation method in a basic media (Sohrabi, Rasouli, & Torkzadeh, 2014). The chitosan has not appropriate functional groups to graft directly onto Fe_3O_4 NPs, thus it should be carboxymethylated and then covalently bound on Fe_3O_4 NPs with carbodiimide activation. This step is as follows:

Solution of chitosan was prepared via dissolving 0.25 g CS in 50 mL of solution of acetic acid 1% (V/V). Then, 2.0 g of Fe_3O_4 NPs that prepared in previous step was added to the CS solution at ambient temperature and stirred for 0.5 h, and then NaOH solution (50 mL, 1.0 M) was added slowly. Finally, the obtained Fe_3O_4-chitosan was collected using external supper magnet and washed by ethanol, distilled water and acetone and kept under vacuum drying.

2.5 Synthesis of the Cu NPs@Fe_3O_4-chitosan

To prepare of the Cu NPs@Fe_3O_4-chitosan, 1.0 g MCS and 0.5 g $CuCl_2.2H_2O$ was mixed with 100 mL aqueous extract and stirred at 80 ºC for 4 h. The produced precipitation was removed by decantation using an external magnet, washed with deionized water and finally dried.

2.6 Synthesis of N-substituted-N-aryl-5-amino-1H-tetrazoles in water

An appropriate cyanamide (1.0 mmol), Cu NPs@Fe_3O_4-chitosan (0.08 g), NaN_3 (1.1 mmol), and water (15 mL) were stirred under reflux conditions. After affirming the end of process by TLC, the catalyst was removed using external supper magnet and 25 mL ethyl acetate and 25 mL HCl (2 M) were added to the mixture reaction. The organic phase was isolated by a separator, and then the resulting aqueous phase was extracted twice with ethyl acetate. The products were obtained via concentration of organic phases and then recrystallization from aqueous ethanol to give pure tetrazoles.

2.7 Spectroscopic data for new compounds

5-(2,4-Dichlorophenyl)amino-1*H*-tetrazole

M.p. 218-220 °C; FT-IR (KBr, cm^{-1}): 3299, 3136, 1658, 1589, 1489, 1392, 1317, 1243, 1135, 1089, 1030, 878, 824, 748, 695, 662, 593, 557, 510, 449; ^{1}H NMR (400 MHz, DMSO-*d*$_6$): δ_H 11.97 (s, 1H), 7.94 (d, *J* = 2.4 Hz, 1H), 7.87 (d, *J* = 8.8 Hz, 1H), 7.61 (d, *J* = 8.8 Hz, 1H), 7.05 (s, 1H); ^{13}C NMR (100 MHz, DMSO-*d*$_6$): δ_C 155.4, 133.5, 132.6, 132.5, 132.1, 126.9, 125.3; Anal. Calcd for $C_7H_5N_5Cl_2$: C, 36.55; H, 2.19; N, 30.44. Found: C, 36.66; H, 2.21; N, 30.55.

***N*-(4-Chlorophenyl)-4-methyl-*N*-(1*H*-tetrazol-5-yl)benzenesulfonamide**

FT-IR (KBr, cm^{-1}): 3471, 3098, 3067, 2981, 1628, 1596, 1487, 1398, 1358, 1307, 1294, 1274, 1244, 1211, 1187, 1162, 1121, 1088, 1039, 1016, 960, 931, 812, 717, 664, 634, 617, 583, 549, 518, 490, 444, 441, 425; ^{1}H NMR (600 MHz, DMSO-*d*$_6$): δ_H 7.67 (d, *J* = 8.2 Hz, 2H), 7.37 (d, *J* = 8.5 Hz, 2H), 7.35 (d, *J* = 8.5 Hz, 2H), 7.18 (d, *J* = 8.2 Hz, 2H), 2.37 (s, 3H); ^{13}C NMR (150 MHz, DMSO-*d*$_6$): δ_C 159.9, 144.0, 138.4, 135.1, 132.0, 129.5, 129.0, 128.2, 21.1; Anal. Calcd for $C_{14}H_{12}ClN_5O_2S$: C, 48.07; H, 3.46; N, 20.02. Found: C, 48.15; H, 3.57; N, 20.13.

4-Bromo-*N*-(4-bromophenyl)-*N*-(1*H*-tetrazol-5-yl)benzenesulfonamide

FT-IR (KBr, cm^{-1}): 3437, 2940, 2921, 1627, 1572, 1481, 1364, 1171, 1068, 1012, 965, 928, 821, 744, 707; ^{1}H NMR (600 MHz, DMSO-*d*$_6$): δ_H 7.82 (d, *J* = 8.6 Hz, 2H), 7.72 (d, *J* = 8.6 Hz, 2H), 7.52 (d, *J* = 8.7 Hz, 2H), 7.14 (d, *J* = 8.7 Hz, 2H); ^{13}C NMR (150 MHz, DMSO-*d*$_6$): δ_C 159.3, 138.7, 137.4, 132.13, 132.10, 130.2, 129.4, 127.5, 120.6; Anal. Calcd for $C_{13}H_9Br_2N_5O_2S$: C, 34.01; H, 1.98; N, 15.25. Found: C, 34.10; H, 2.09; N, 15.34.

4-Bromo-*N*-(4-chlorophenyl)-*N*-(1*H*-tetrazol-5-yl)benzenesulfonamide

FT-IR (KBr, cm^{-1}): 3105, 3063, 1645, 1591, 1575, 1516, 1485, 1471, 1411, 1390, 1375, 1353, 1339, 1304, 1286, 1275, 1239, 1203, 1180, 1172, 1111, 1087, 1068, 1062, 1038, 1016, 1010, 987, 965, 929, 827, 818, 784, 744, 722, 710, 699, 670, 633, 612, 566, 520, 497, 490, 454, 440; ^{1}H NMR (600 MHz, DMSO-*d*$_6$): δ_H 7.89 (d, *J* = 8.7 Hz, 2H), 7.70 (d, *J* = 8.7 Hz, 2H), 7.28 (d, *J* = 8.7 Hz, 2H), 7.52 (d, *J* = 8.7 Hz, 2H); ^{13}C NMR (150 MHz, DMSO-*d*$_6$): δ_C 157.7, 136.2, 135.9, 133.9, 132.7, 130.3, 130.2, 129.8, 128.7; Anal. Calcd for $C_{13}H_9BrClN_5O_2S$: C, 37.66; H, 2.19; N, 16.89. Found: C, 37.78; H, 2.22; N, 17.01.

3. Results and discussion

In this study, a simple process for the preparation of the Cu NPs@Fe_3O_4-chitosan is presented via in situ decoration of Cu NPs on the Fe_3O_4-chitosan substrate biosupport in presence of *E. falcate* leaf extract (Scheme 3). The easy synthetic procedure afforded catalyst and its catalytic prowess was investigated for the synthesis of a variety of tetrazoles.

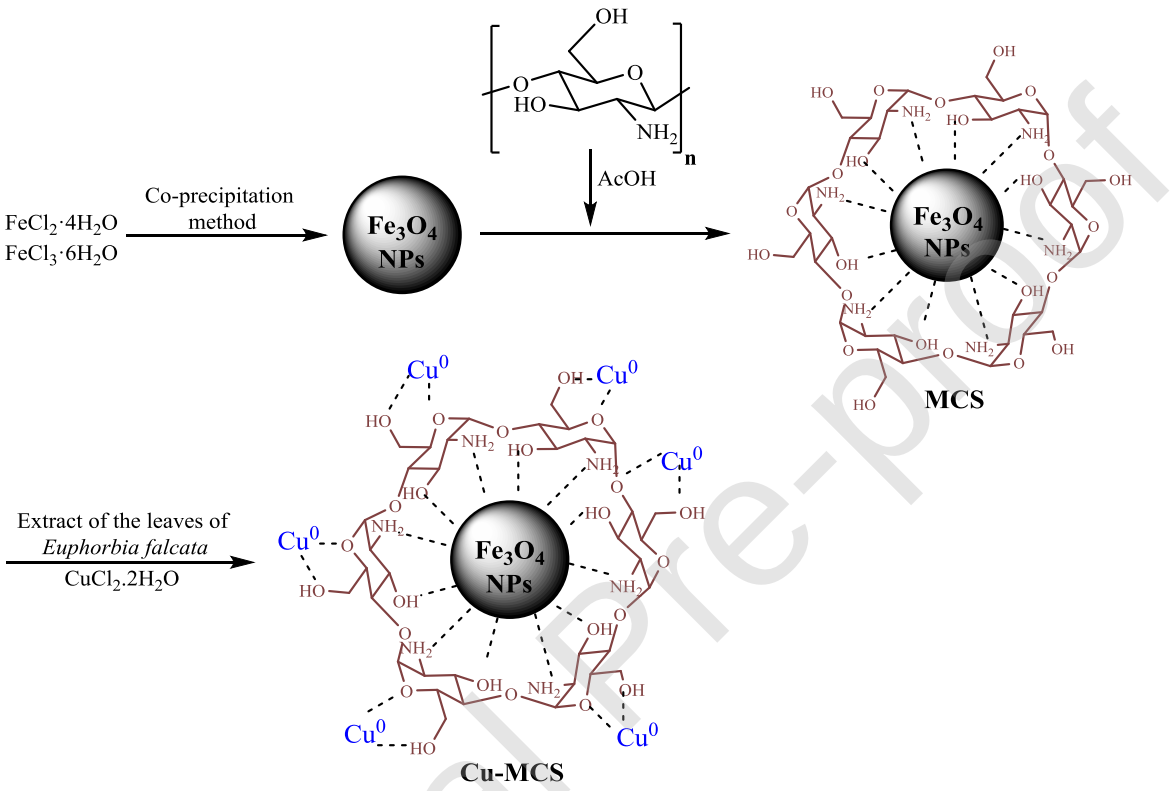

Scheme 3. Procedure for the preparation of Cu NPs@Fe_3O_4-chitosan.

3.1 Characterization of extract and the catalyst

The phytochemical study of *E. falcata* extract was previously described (Sulyok, Vasas, Rédei, Forgo, Kele, Pinke, & Hohmann, 2011). *E. falcata* phytochemical constituents include antioxidant phenolics such as quercetin, kaempferol and rutin as aglycones or bearing sugar moieties and can be used for biological synthesis of Cu NPs. Four diterpenes were isolated via the method introduced by Sulyok *et al*. from the *E. falcata* extract by a combination of different chromatographic methods. First, the synthesis of the Cu NPs (Scheme S1) was performed using polyphenolics of extract as reducing/stabilizing agents.

Figure S1 shows peaks at 235 and 351 nm owing to benzoyl and cinnamoyl systems, respectively (Bhat, Nagasampagi, & Sivakumar, 2005). Moreover, Figure S2 described the changes in the maximum absorbance of Cu^{2+}

ions undergo SPR phenomenon and Cu NPs production. Further, the stability of synthesized NPs was investigated to 15 days using UV-Vis spectroscopy. The FT-IR analysis of the crude extract (Figure S3) showed signals in 3400, 1715 and 1445 cm^{-1} which represent stretching vibrations of OH, C=O and C=C, respectively as the functional groups of phenolics. The FT-IR analysis of Cu NPs depicted the signals around 3500, 1725, 1428, 1300 to1000 cm^{-1} represent the stretching vibrations of OH, C=O, C=C and C-OH, respectively (Figure S4). The nanoparticles stability refers to the adsorbed polyphenolics on the Cu NPs surface. Cu NPs structure was ascertained by XRD (Figure S5). The peaks located at 43.4° (111), 50.8° (200) and 74.5° (220) are assigned to Cu NPs.

3.2 Characterization of Cu NPs@Fe_3O_4-chitosan

The structure of Cu NPs@Fe_3O_4-chitosan was thoroughly characterized using powder XRD, FESEM, EDS, TEM, STEM, elemental mapping, VSM, TG/DTG and FT-IR spectroscopy. Figure S6 depicts the Cu NPs@Fe_3O_4-chitosan FT-IR. The broad peak at 3400 cm^{-1} could be related to the stretching vibrations of -OH and/or -NH in chitosan, while weak peaks around 2935 cm^{-1} could be pertinent to the asymmetric stretch of -CH group (Liu, Wang, Liu, Jiang, Yu, Mu, & Wang, 2012). The signals at 1623, 1564 and 1261 cm^{-1} related to stretching vibrations of C=O in the amide I, -NH bending and C-N stretching in amide II and N-H bending and the C-N stretching bands in the amide III, respectively. The signals at 1385 and 1069 cm^{-1} corresponded to CH_2OH of C-6 position and O-H bending of the sugar piece of chitosan, respectively (Mansur, Mansur, Curti, & De Almeida, 2013). The peak related to C-O-C nonsymmetric stretching and glycoside linkage of saccharide structure, appeared in order at 1151 and 892 cm^{-1} (Zhang, Jiang, Ma, Cai, Zhou, & Wang, 2011). The signal at 634 cm^{-1} attributed to the Fe-O bond vibrating of iron oxide nanoparticles.

The presence of Cu and Fe_3O_4 was verified with XRD analysis. Six separately Bragg peaks are depicted in Figure 1 at 30.2, 35.8, 43.5, 53.7, 57.2, 62.8 corresponding to 220, 311, 400, 511, 440, and 533 Bragg reflection planes (JCPDS file, PDF No. 65-3107). It indicates that the magnetic Fe_3O_4 nanoparticles has been successfully combined with CS. On the other hand, the diffraction peaks for Cu NPs appeared at 43.4, 50.8 and 74.5 assigning to the 111, 200 and 220 planes, respectively. Figure 2 shows morphology of the Cu NPs@Fe_3O_4-chitosan according to SEM analysis. FESEM images were confirmed that the Cu NPs were attached to the substrate of the magnetic chitosan.

The chemical composition and Cu NPs distribution in the green synthesized Cu NPs@Fe_3O_4-chitosan was characterized by EDS and elemental mapping (Figure 3). In EDS spectrum, Cu, Fe, O, N and C peaks were observed,

indicating the authenticity of Cu NPs@Fe_3O_4-chitosan. As shown in Figure 3, the Cu NPs@Fe_3O_4-chitosan elemental mapping was verified the Cu NPs distribution on the magnetic CS surface.

The Cu NPs@Fe_3O_4-chitosan TEM analysis (Figure 4) displayed the decoration of the Cu NPs on the magnetic CS surface, comprising Cu NPs and magnetic CS with the average size of 5-10 and ~50 nm, respectively with spherical morphology.

The HRTEM and fast Fourier transform (FFT) image of the nanocomposite catalyst show that both Fe_3O_4 and Cu nanoparticles are highly crystalline (Figure 5a-c). STEM image confirms a homogeneously assembled nanostructured catalyst (Figure 5d).

TG/DTG analysis was applied to examine the Cu NPs@Fe_3O_4-chitosan thermal stability (Figure S7). The mass loss happens up to 200 °C is ascribed to the loss of molecules moisture and physically adsorbed solvent. The weight loss high 200°C is associate to polysaccharide chain thermal decomposition. So, the above temperature for chitosan decomposition shown the elevated thermal stability of the catalyst. The magnetic property of the nanocomposite catalyst was studied using a VSM magnetometer (Figure S8) demonstrating an outstanding magnetic separation for effective recycling of the catalyst.

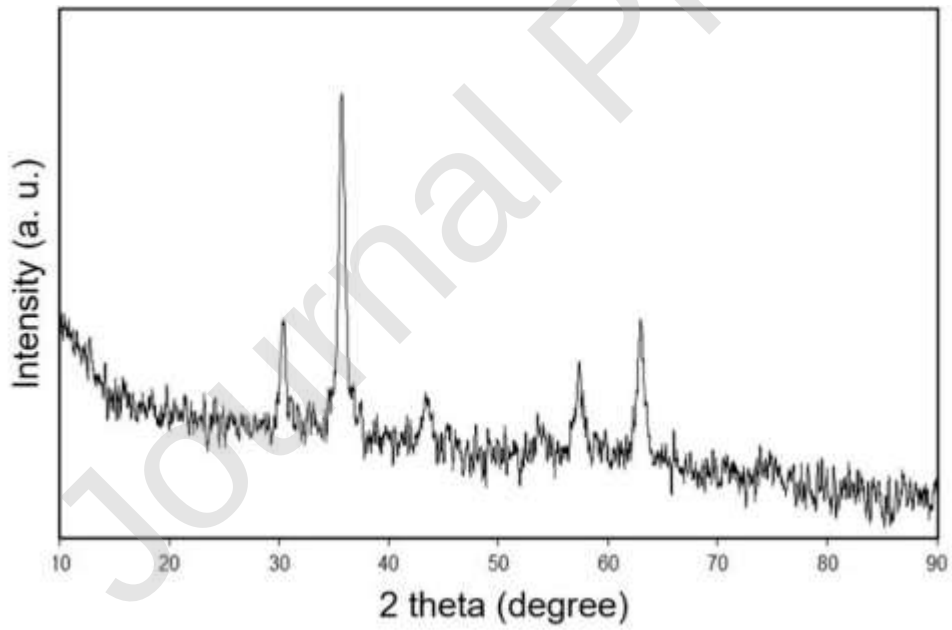

Figure 1. XRD pattern of the Cu NPs@Fe_3O_4-chitosan.

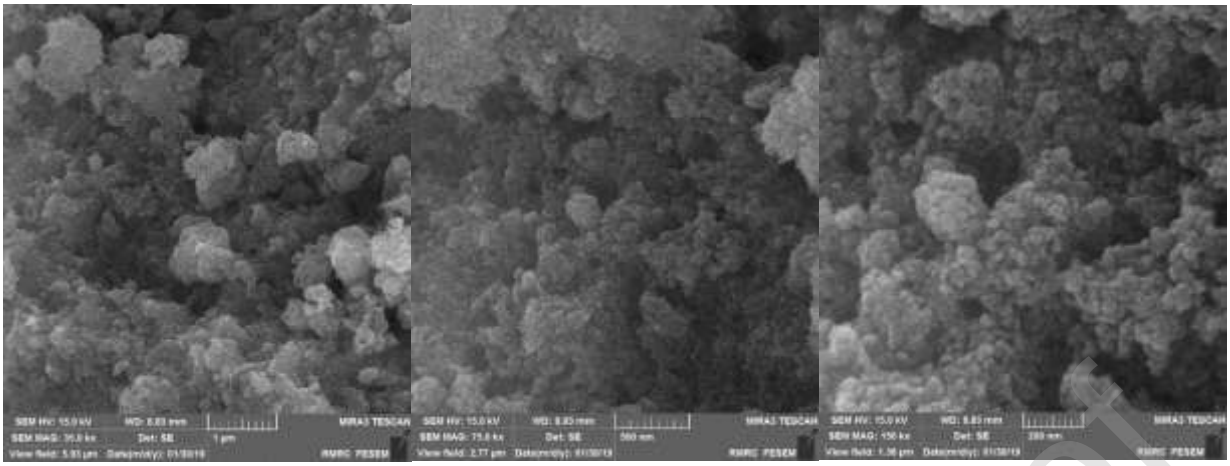

Figure 2. FESEM analysis of the Cu NPs@Fe_3O_4-chitosan.

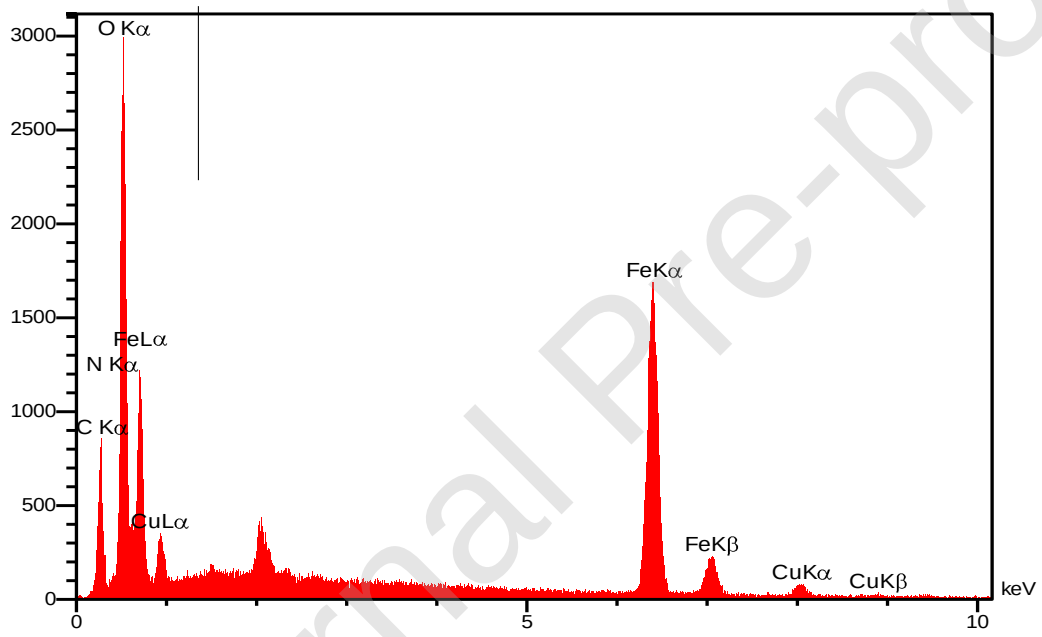

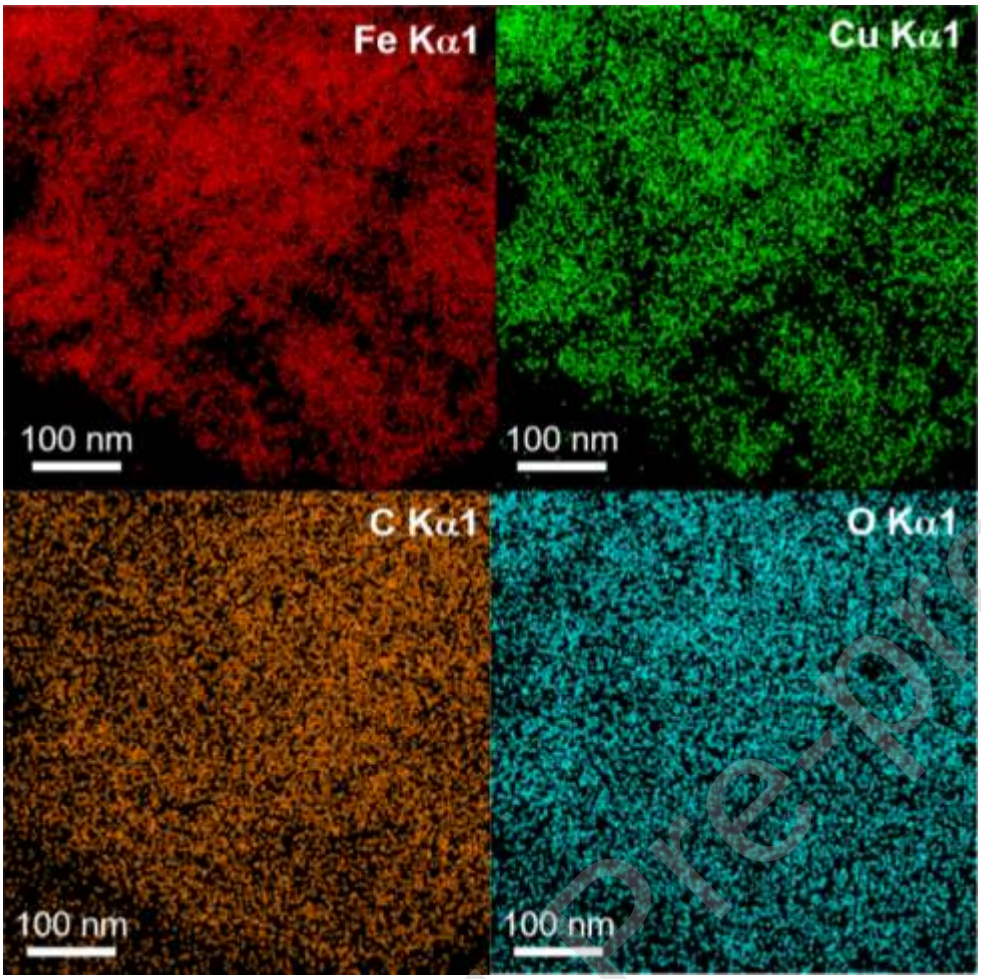

Figure 3. EDS spectrum and elemental mapping of the Cu NPs@Fe_3O_4-chitosan.

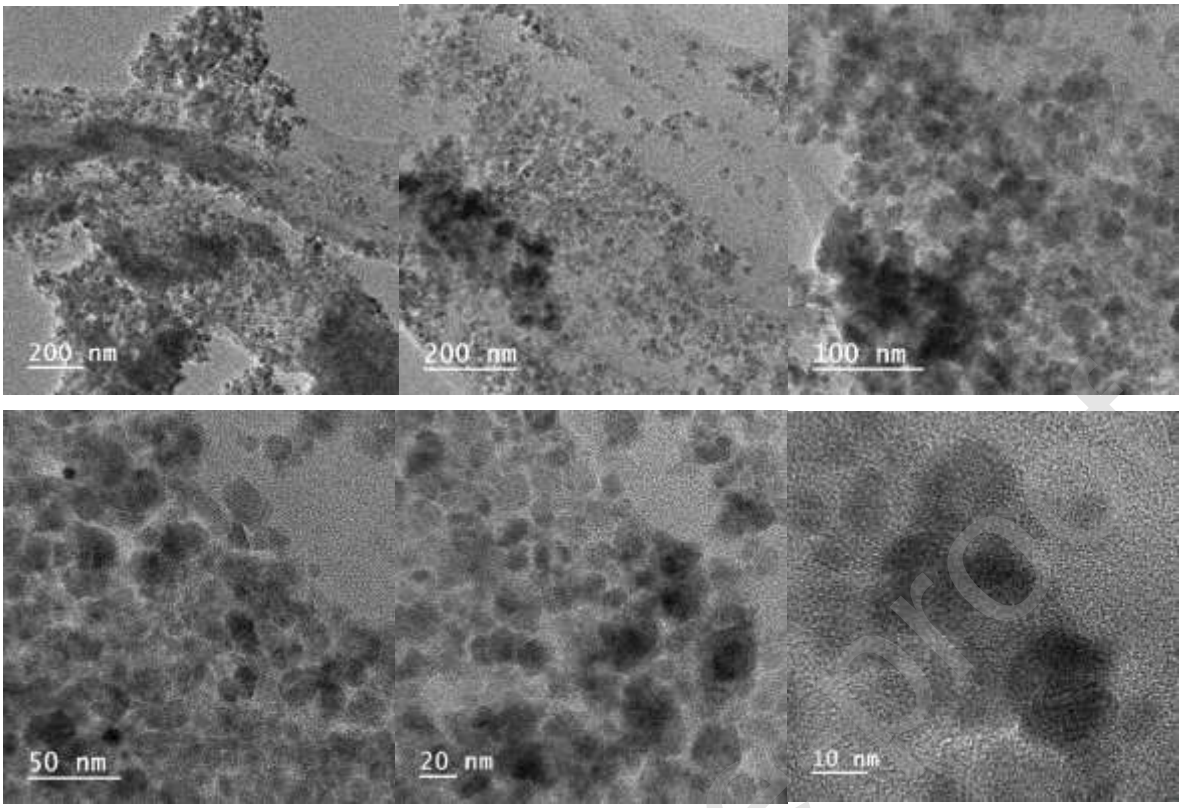

Figure 4. TEM images of the Cu NPs@Fe_3O_4-chitosan.

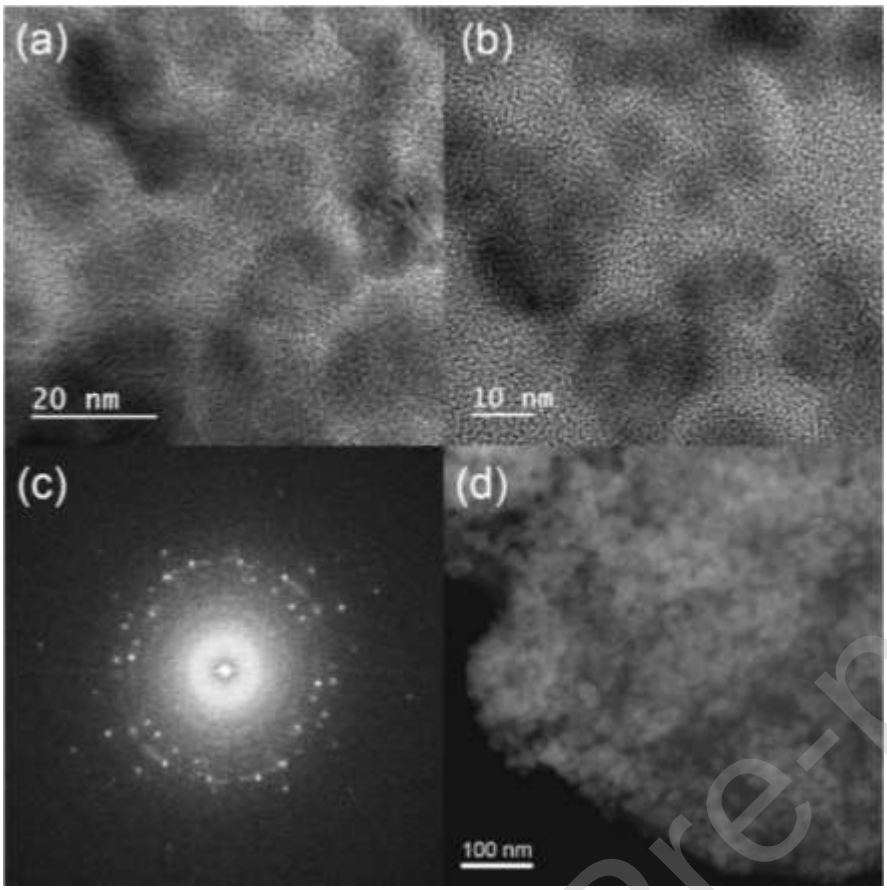

Figure 5. (a, b) HRTEM, (c) FFT and STEM images of the Cu NPs@Fe_3O_4-chitosan.

3.3 Preparation various tetrazoles using Cu NPs@Fe_3O_4-chitosan catalyst

2,4-Dimethylphenylcyanamide and NaN_3 were selected for the initial exploratory investigation (Table 1). Notably, the reaction led to clean conversion when conducted in water as a green solvent and catalyzed by Cu NPs@Fe_3O_4-chitosan. The efficiency of catalyst loading on the production of product was studied by different quantities of catalyst. As shown in entry 1, the product was not obtained in the absence of the Cu NPs@Fe_3O_4-chitosan. When 0.03 g of the catalyst is used as the catalyst, 78% yield of product is attained (entry 2). This high yield indicates that Cu NPs@Fe_3O_4-chitosan acts as an effective catalyst for the synthesis of tetrazole; 0.04, 0.06 and 0.08 g of catalyst, afforded 81, 84 and 88 %, respectively. No further improvement in the yield of reaction discerned by increasing the amount to 0.1 g (entry 7).

Based on the optimized conditions, we investigated the effect of various substituents on the cyanamides aromatic ring. Essentially, the Cu NPs@Fe_3O_4-chitosan displayed high catalytic activity for the reaction of various *N*-arylcyanamides possessing diverse functionalities with NaN_3 in water and corresponding tetrazoles were prepared in

high yields (Table 2). There is an excellent interrelationship between substituent type and outcome for the product. According to the obtained results, **B** and **A** isomers can be produced from *N*-arylcyanamides carrying electron-donating and electron-withdrawing groups, respectively via the formation of guanidine azide intermediate (Scheme S2). According to the documented results in the literature, in most cases, isomeric mixtures was observed in the synthesis of tetrazoles from cyanamides, while the present method was completely regiospecific (Scheme S3). The regiospecificity of cyanamides reaction with NaN_3 provides a novel process for the synthesis of specific type of tetrazole (**A** or **B**).

Commonly, when the substitution on the cyanamides ring in *ortho* position is Cl (Table 2, entries 9-12), the formation of **A** isomer is favoured owing to the intramolecular hydrogen bonding between Cl and NH amine group (Scheme S4).

We have also assessed the catalytic prowess of Cu NPs@Fe_3O_4-chitosan for the synthesis of *N*-sulfonyl-*N*-aryl-5-amino-1*H*-tetrazoles for the first time from corresponding cyanamides in refluxing water conditions (Table 2, entries 17-19). As shown in Table 2, compared to **B** and **A** isomers, *N*-sulfonyl-*N*-aryl-5-amino-1*H*-tetrazoles preparation required longer reaction times owing to sulfonyl groups presence on the nitrogen atom in *N*-sulfonyl-*N*-arylcyanamides.

To indicate the comparative efficacy of our method, Scheme S5 show comparison of designed Cu NPs@Fe_3O_4-chitosan with reported catalysts in the literature for the [2+3] cycloaddition between 2,4-dichlorophenylcyanamide and NaN_3 (Henry, Finnegan, & Lieber, 1954; Herr, 2002; Katritzky, Rees, & Scriven, 1996; Nasrollahzadeh, Sajjadi, Komber, Khonakdar, & Sajadi, 2019; Peet, Baugh, Sundler, Lewis, Matthews, Olberding, & Shah, 1986; Singh, Chawla, Kapoor, Paul, & Malhotra, 1980). As shown in Scheme S5, Cu NPs@Fe_3O_4-chitosan catalyst is a more efficient catalyst than previously reported ones from the view point of product yield, regiospecificity, reaction time, and used solvent. The following disadvantages, observed in reported protocols in the literature for the synthesis of tetrazoles, were overcome; none of the listed drawbacks are found in our protocol for this regiospecific reaction:

- The employment of harmful solvents and dangerous HN_3
- *In situ* preparation of HN_3
- Low regiospecificity of reaction (production of isomers mixture)
- Low product yields
- Great reaction times

- The use of high amounts of homogeneous catalysts without recyclability
- Difficulties in availability of the natural zeolite

Table 1. Optimization of synthesis of 5-(2,4-dimethylphenyl)amino-1*H*-tetrazole.[a]

Entry	Cu NPs@Fe_3O_4-chitosan (g)	Time (h)	d (%)[b]
1	0.0	24	0.0
2	0.03	10	78
3	0.04	8.5	81
4	0.06	7	84
5	0.08	5.5	88
6	0.1	5.5	88

[a]Reaction conditions: 2,4-dimethylphenylcyanamide (1.0 mmol); NaN_3 (1.1 mmol) and H_2O (15 mL), reflux.

[b]Isolated yield.

Table 2. Synthesis of tetrazoles by Cu NPs@Fe_3O_4-chitosan.[a]

Entry	Substrate	Product	Time (h)	Yield%[a]
1	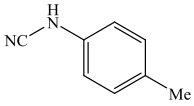	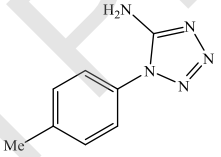	5.5	88
2	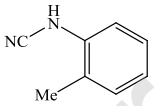	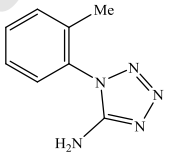	5.5	87
3	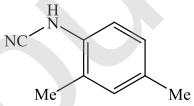	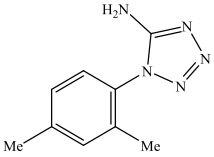	5.5	88
4	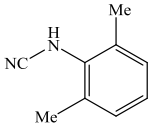	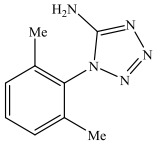	5.5	83

5	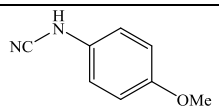	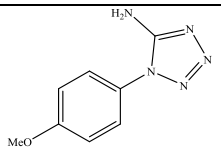	5.5	86
6	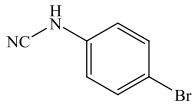	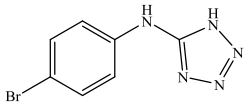	6	90
7	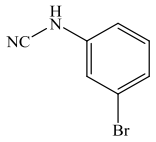	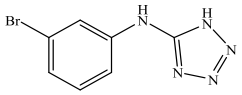	6	87
8	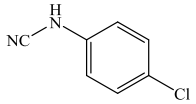	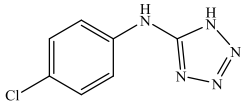	6	87
9	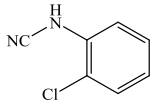	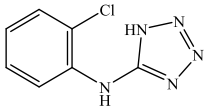	6	85
10	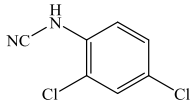	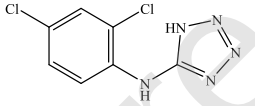	6	86
11	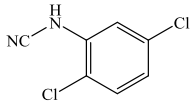	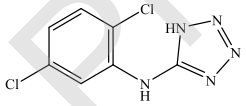	6	87
12	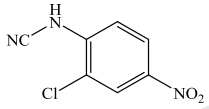	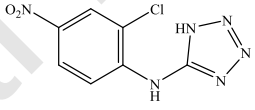	7	82
13	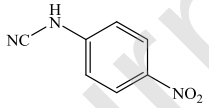	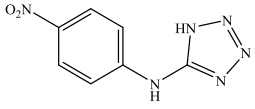	7	81
14	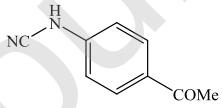	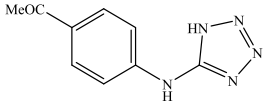	7	82
15	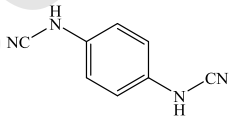	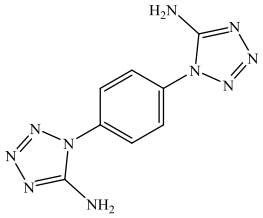	4.5	85

16	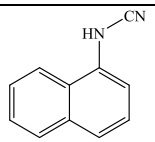	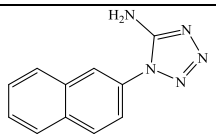	6	86
17	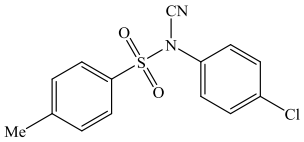	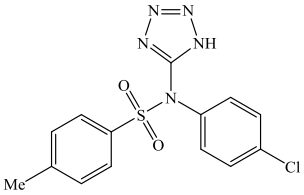	22	83
18	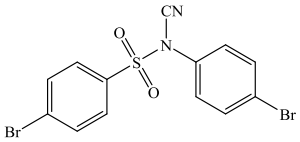	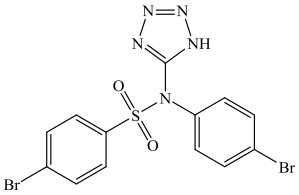	22	82
19	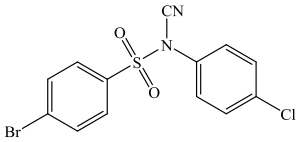	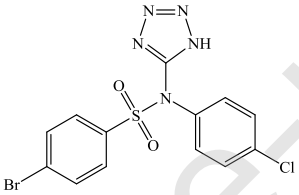	22	82

[a] Reaction conditions: Cyanamide derivative (1.0 mmol), NaN_3 (1.1 mmol), H_2O (15 mL), catalyst (0.08 g), reflux.

[b]Isolated yield of the pure product.

The structure of tetrazoles were confirmed by ^{1}HNMR, ^{13}CNMR, elemental (CHN) analysis and FT-IR analyses. The conversion of cyanamides to tetrazoles could be monitored using FT-IR spectroscopy. After the tetrazole formation, CN stretching band in cyanamide structure disappeared with the appearance of two stretching bands corresponding to NH groups which confirmed the formation of tetrazole (Figure S9 and S10). The ^{1}HNMR spectrum of **A** isomer shows two NH signals corresponding to tetrazole ring (NH^T) and amine group bonded with aryl ring (NH^A)) (Figure S11), while the ^{1}HNMR spectrum of **B** isomer was characterized *via* appearance of one NH_2 peak. The ^{13}CNMR spectrum confirmed the tetrazole formation *via* appearance of peak at δ = 154-159 ppm concerning carbon of tetrazole ring (Figure S12).

3.4 Catalyst recyclability

The Cu NPs@Fe_3O_4-chitosan reusability for the synthesis of tetrazoles was studied using the reaction of 2-chlorophenylcyanamide with NaN_3; the Cu NPs@Fe_3O_4-chitosan catalyst could be simply removed from the reaction deploying an external magnetic field, washed twice by ethanol, dried at 100 °C for 5 h and finally was used again for the next catalytic run. Interestingly, this nanocatalyst can be reused five times without significant decrease in the catalytic ability (Figure S13). Moreover, the integrity of the recycled Cu NPs@Fe_3O_4-chitosan in terms of size, shape and chemical composition after the 5th run was verified by FESEM (Figure S14), EDS (Figure S15) analysis and elemental mapping (Figure S16) and TEM (Figure S17). The experimental results display that the magnetic chitosan play an essential role in the stabilization of Cu NPs and prevent their agglomeration, thus minimizing the leaching of Cu species during the reaction. According to the studies conducted using ICP-MS analysis in the present work, less than 0.1% of the Cu was observed in the solution during cycloaddition.

4. Conclusions

In this research, a proficient magnetic NPs-supported Cu adorned on the surface of chitosan modified with Fe_3O_4 NPs. Cu NPs were simply synthesized and immobilized on the magnetic chitosan using *E. falcata* leaf extract as stabilizing and reducing agent for the preparation of Cu NPs@Fe_3O_4-chitosan without of use of poisonous reducing agents. FESEM, XRD, EDS, TEM, VSM, TG/DTG, STEM, elemental mapping and FT-IR techniques were applied for the confirmation of the Cu NPs@Fe_3O_4-chitosan. FT-IR analysis of extract indicated the presence of flavonoids or polyphenols in the *E. falcata* which are responsible for Cu^{2+} ions reduction. The Cu NPs@Fe_3O_4-chitosan showed excellent catalytic efficiency for the synthesis of various tetrazoles in high yields. This synthetic procedure has numerous benefits of high yields, avoidance of the preparation and use of hazardous and harmful hydrazoic acid, easy work-up procedure, use of water as an eco-friendly solvent instead of toxic solvents such as DMF with the added advantage of catalyst stability and reusability.

Acknowledgement

The support of this work by the University of Qom and the Iranian Nano Council is greatly appreciated.

References

Frija, L.M.T., Cristiano, M.L.S., Gómez-Zavaglia, A., Reva, I., & Fausto, R. (2014). Genesis of rare molecules using light-induced reactions of matrix-isolated tetrazoles. *J. Photochem. Photobiol. C Photochem. Rev*., *18*, 71-90.

Frija, L.M.T., Ismael, A., & Cristiano, M.L.S. (2010). Photochemical transformations of tetrazole derivatives: applications in organic synthesis. *Molecules*, *15*, 3757-3774.

Ichinari, D., Nagaki, A., & Yoshida, J.I. (2017). Generation of hazardous methyl azide and its application to synthesis of a key-intermediate of picarbutrazox, a new potent pesticide in flow. *Bioorg. Med. Chem*., *25*, 6224-6228.

Koldobskii, G.I. (2006). Strategies and prospects in functionalization of tetrazoles. *Russ. J. Org. Chem*., *42*, 469-486.

Nasrollahzadeh, M., Sajjadi, M., & Khonakdar, H.A. (2018). Synthesis and characterization of novel Cu (II) complex coated Fe_3O_4@SiO_2 nanoparticles for catalytic performance. *J. Mol. Struct*., *1161*, 453-463.

Ostrovskii, V.A., Popova, E.A., & Trifonov, R.E. (2017). Developments in tetrazole chemistry (2009-16). *Adv. Heterocycl. Chem*., *123*, 1.

Pino-Gonzalez, M.S., Romero-Carrasco, A., Calvo-Losada, S., Oña-Bernal, N., Quirante, J.J., & Sarabia, F. (2017). Synthesis of tetrazole fused azepanes and quantum chemical topology study on the mechanism of the intramolecular cycloaddition reaction. *RSC Adv*., *7*, 50367-50371.

Wei, C.X., Bian, M., & Gong, G.H. (2015). Tetrazolium compounds: synthesis and applications in medicine. *Molecules*, *20*, 5528-5553.

Burger, A. (1991), Isosterism and bioisosterism in drug design. *Prog. Drug. Res*., *37*, 287-371.

Gutmann, B., Glasnov, T., Razzaq, T., Goessler, W., Roberge, D.M., & Kappe, C.O. (2011). Unusual behavior in the reactivity of 5-substituted-1*H*-tetrazoles in a resistively heated microreactor. *Beilstein J. Org. Chem*., *7*, 503-517.

Arshad, M., Bhat, A.R., Pokharel, S., Kim, J.E., Lee, E.J., Athar, F., & Choi, I. (2014). Synthesis, characterization and anticancer screening of some novel piperonyl-tetrazole derivatives. *Eur. J. Med. Chem*., *71*, 229-236.

ElMonaem, H.S.A., Abdel-Aziz, N.I., Morsy, M.A., Badria, F.A., ElSenduny, F., El-Ashmawy, M.B., & Moustafa, M.A. (2016). Synthesis, In Vitro Antiproliferative Evaluation and Molecular Docking of New tetrazole-chalcone and tetrazole-pyrazoline Hybrids. *J. Am. Sci*., *12*, 40-56.

Sajjadi, M., Nasrollahzadeh, M., & Sajadi, S.M. (2017). Green synthesis of Ag/Fe_3O_4 nanocomposite using Euphorbia peplus Linn leaf extract and evaluation of its catalytic activity. *J. Colloid Interface Sci*., *497*, 1-13.

Schmidt, B., & Schieffer, B. (2003). Angiotensin II AT1 receptor antagonists. Clinical implications of active metabolites. *J. Med. Chem*., *46*, 2261-2270.

Tanaka, T., Okuda, T., & Yamamoto, Y. (2004). Characterization of the CYP3A4 active site by homology modeling. *Chem. Pharm. Bull*., *52*, 830-835

Wexler, R.R., Greenlee, W.J., Irvin, J.D., Goldberg, M.R., Prendergast, K., Smith, R.D., & Timmermans, P.B. (1996). Nonpeptide angiotensin II receptor antagonists: the next generation in antihypertensive therapy. *J. Med. Chem*., *39*, 625-656.

Henry, A.R., Finnegan, W.G., & Lieber, E. (1954). Thermal isomerization of substituted 5-aminotetrazoles. *J. Am. Chem. Soc*., *76*, 88-93.

Herr, R.J. (2002). 5-Substituted-1H-tetrazoles as carboxylic acid isosteres: medicinal chemistry and synthetic methods. *Bioorg. Med. Chem*., *10*, 3379-3393.

Katritzky, A.R., Rees, C.W., & Scriven, E.F. (1996). In *Comprehensive Heterocyclic Chemistry II*, New York, NY, Vol. 4, p. 621.

Peet, N.P., Baugh, L.E., Sundler, S.L., Lewis, E., Matthews, E.H., Olberding, E.L., & Shah, D.N. (1986). 3-(1H-Tetrazol-5-yl)-4(3H)-quinazolinone sodium salt (MDL 427): a new antiallergic agent. *J. Med. Chem*., *29*, 2403-2409.

Singh, H., Chawla, A.S., Kapoor, V.K., Paul, D., & Malhotra, P.K. (1980). Medicinal chemistry of tetrazoles. Progress in medicinal chemistry of tetrazoles. *Prog. Med. Chem*., *17*, 151-183.

Miller, A.E., Feeney, D.J., Ma, Y., Zarcone, L., Aziz, M.A., & Magnuson, E. (1990). The synthesis of aminoiminoethanenitriles, 5-aminotetrazoles, N-cyanoguanidines, and N-hydroxyguanidines from aminoiminomethanesulfonic acids. *Synth. Commun*., *20*, 217-226.

Nasrollahzadeh, M., Sajjadi, M., Komber, H., Khonakdar, H. A., & Sajadi, S. M. (2019). In situ green synthesis of Cu- Ni bimetallic nanoparticles supported on reduced graphene oxide as an effective and recyclable catalyst for the synthesis of *N*- benzyl- *N*- aryl- 5- amino- 1*H*- tetrazoles. *Appl. Organomet. Chem*., *33*, e4938.

Congreve, M.S. (1996). Synthesis of 5-N-Substituted Tetrazole Derivatives of the Potent NK1 Receptor Antagonist GR203040. *Synlett*, 359-360.

Garbrecht, W.L., & Herbst, R.M. (1953). The synthesis of certain 5-aminotetrazole derivatives. II. The action of hydrazoic acid on monoalkylcyanamides. *J. Org. Chem*., *18*, 1014-1021.

Habibi, D., Nasrollahzadeh, M., Faraji, A.R., & Bayat, Y. (2010). Efficient synthesis of arylaminotetrazoles in water. *Tetrahedron*, *66*, 3866-3870.

Henry, R.A., Finnegan, W.G., & Lieber, E. (1955). Kinetics of the isomerization of substituted 5-aminotetrazoles. *J. Am. Chem. Soc*., 77, 2264-2270.

Nasrollahzadeh, M., Habibi, D., Shahkarami, Z., & Bayat, Y. (2009). A general synthetic method for the formation of arylaminotetrazoles using natural natrolite zeolite as a new and reusable heterogeneous catalyst. *Tetrahedron*, *65*, 10715-10719.

Vorobiey, A.N., Gaponik, P.N., Petrov, P.T., & Ivashkevich, O.A. (2006). One-pot syntheses of 5-amino-1-aryltetrazole derivatives. *Synthesis*, 1307-1312.

Modarresi-Alam, A.R., & Nasrollahzadeh, M. (2009). Synthesis of 5-arylamino-1*H* (2H)-tetrazoles and 5-amino-1-aryl-1H-tetrazoles from secondary arylcyanamides in glacial acetic acid: a simple and efficient method. *Turk. J. Chem*., *33*, 267-280.

Habibi, D., & Nasrollahzadeh, M. (2010). Silica-supported ferric chloride ($FeCl_3$-SiO_2): an efficient and recyclable heterogeneous catalyst for the preparation of arylaminotetrazoles. *Synth. Commun*., *40*, 3159-3167.

Yella, R., Khatun, N., Rout, S.K., & Patel, B.K. (2011). Tandem regioselective synthesis of tetrazoles and related heterocycles using iodine. *Org. Biomol. Chem*., *9*, 3235-3245.

Baig, R.N., Nadagouda, M.N., & Varma, R.S. (2014). Carbon-coated magnetic palladium: applications in partial oxidation of alcohols and coupling reactions. *Green Chem*., *16*, 4333-4338.

Li, M., & Guan, J. (2017). Heterogeneous Catalysts in Organic Synthesis: From Nanoscale to Single Atomic Level. *Adv. Org. Synth*., *7*, 228-258.

Polshettiwar, V., & Varma, R.S. (2009) Nanoparticle-supported and magnetically recoverable palladium (Pd) catalyst: a selective and sustainable oxidation protocol with high turnover number. *Org. Biomol. Chem*., *7*, 37-40.

Rathi, A.K., Gawande, M.B., Pechousek, J., Tucek, J., Aparicio, C., Petr, M., & Zboril, R. (2016). Maghemite decorated with ultra-small palladium nanoparticles (γ-Fe_2O_3-Pd): applications in the Heck-Mizoroki olefination, Suzuki reaction and allylic oxidation of alkenes. *Green Chem*., *18*, 2363-2373.

Wang, Y., Li, Q., Zhang, P., O'Connor, D., Varma, R.S., Yu, M., & Hou, D. (2018). One-pot green synthesis of bimetallic hollow palladium-platinum nanotubes for enhanced catalytic reduction of *p*-nitrophenol. *J. Colloid Interface Sci*., *539*, 161-167.

Gawande, M.B., Branco, P.S., & Varma, R.S. (2013). Nano-magnetite (Fe_3O_4) as a support for recyclable catalysts in the development of sustainable methodologies. *Chem. Soc. Rev*., *42*, 3371-3393.

Hu, W., Liu, B., Wang, Q., Liu, Y., Liu, Y., Jing, P., & Zhang, J. (2013). A magnetic double-shell microsphere as a highly efficient reusable catalyst for catalytic applications. *Chem. Commun*., *49*, 7596-7598.

Oi, L.E., Choo, M.Y., Lee, H.V., Ong, H.C., Hamid, S.B.A., & Juan, J.C. (2016). Recent advances of titanium dioxide (TiO_2) for green organic synthesis. *RSC Adv*., *6*, 108741-108754.

Sharma, R. K., Dutta, S., Sharma, S., Zboril, R., Varma, R. S., & Gawande, M. B. (2016). Fe_3O_4 (iron oxide)-supported nanocatalysts: synthesis, characterization and applications in coupling reactions. *Green Chem*., *18*(11), 3184-3209.

Titirici, M.M., White, R.J., Brun, N., Budarin, V.L., Su, D.S., del Monte, F., & MacLachlan, M.J. (2015). Sustainable carbon materials. *Chem. Soc. Rev*., *44*, 250-290.

Varma, R.S. (2016). Greener and sustainable trends in synthesis of organics and nanomaterials. *ACS Sustainable Chem. Eng*., *4*, 5866-5878.

Xu, L., & Wang, J. (2012). Magnetic nanoscaled Fe_3O_4/CeO_2 composite as an efficient Fenton-like heterogeneous catalyst for degradation of 4-chlorophenol. *Environ. Sci. Technol*., *46*, 10145-10153.

Krajewska, B. (2004). Application of chitin-and chitosan-based materials for enzyme immobilizations: a review. *Enzyme Microb. Technol*., *35*, 126-139.

Lee, M., Chen, B.Y., &B Den, W. (2015). Chitosan as a natural polymer for heterogeneous catalysts support: a short review on its applications. *Appl. Sci*., *5*, 1272-1283.

Banerjee, P., Satapathy, M., Mukhopahayay, A., & Das, P. (2004). Leaf extract mediated green synthesis of silver nanoparticles from widely available Indian plants: synthesis, characterization, antimicrobial property and toxicity analysis. *Bioresour. Bioprocess*, *1*, 3.

Kou, J., & Varma, R.S. (2012). Beet juice utilization: Expeditious green synthesis of noble metal nanoparticles (Ag, Au, Pt, and Pd) using microwaves. *RSC Adv*., *2*, 10283-10290.

Nadagouda, M.N., & Varma, R.S. (2008). Green synthesis of silver and palladium nanoparticles at room temperature using coffee and tea extract. *Green Chem*., *8*, 859-862.

Plachtová, P., Medříková, Z., Zbořil, R., Tuček, J., Varma, R.S., & Maršálek, B. (2018). Iron and iron oxide nanoparticles synthesized with green tea extract: differences in ecotoxicological profile and ability to degrade malachite green. *ACS Sustainable Chem. Eng*., *6*, 8679-8687.

Varma, R.S. (2014). Journey on greener pathways: from the use of alternate energy inputs and benign reaction media to sustainable applications of nano-catalysts in synthesis and environmental remediation. *Green Chem*., *16*, 2027-2041.

Varma, R.S. (2012). Greener approach to nanomaterials and their sustainable applications. *Curr. Opin. Chem. Eng*., *1*, 123-128.

Narayanan, K.B., & Sakthivel, N. (2011). Green synthesis of biogenic metal nanoparticles by terrestrial and aquatic phototrophic and heterotrophic eukaryotes and biocompatible agents. *Adv. Colloid. Interface Sci*., 169, 59-79.

Abdel-Halim, E.S., El-Rafie, M.H., & Al-Deyab, S.S. (2011). Polyacrylamide/guar gum graft copolymer for preparation of silver nanoparticles. *Carbohydr. Polym*., 85, 692-697.

Qazi, F., Hussain, Z., & Tahir, M.N. (2016). Advances in biogenic synthesis of palladium nanoparticles. *RSC Adv*., 6, 60277-60286.

Citoğlu, G.S.T., & Özbilgin, S. (2012). Uses of some Euphorbia species in traditional medicine in Turkey and AAtheir biological activities. *Turk. J. Pharm. Sci*., *9*, 241-256.

Irshad, A., Rubina, N., Wahib, N.K., Rukhsana, G., & Choudhary, M.I. (2009). Biological screening of different root extracts of *Euphorbia wallichii*. *Pak. J. Bot.*, *41*, 1737-1741.

Noori, M., Chehreghani, A., & Kaveh, M. (2009). Flavonoids of 17 species of Euphorbia, (Euphorbiaceae) in Iran. *Toxicol. Environ. Chem.*, *91*, 631-641.

El Bribri, A., Tabyaoui, M., Tabyaoui, B., El Attari, H., & Bentiss, F. (2013). The use of *Euphorbia falcata* extract as eco-friendly corrosion inhibitor of carbon steel in hydrochloric acid solution. *Mater. Chem. Phys*., *141*, 240-247.

Sohrabi, N., Rasouli, N., & Torkzadeh, M. (2014). Enhanced stability and catalytic activity of immobilized α-amylase on modified Fe_3O_4 nanoparticles. *Chem. Eng. J*., *240*, 426-433.

Sulyok, E., Vasas, A., Rédei, D., Forgo, P., Kele, Z., Pinke, G., & Hohmann, J. (2011). New premyrsinane-type diterpene polyesters from *Euphorbia falcata*. *Tetrahedron*, *67*, 7289-7293.

Bhat, S.V., Nagasampagi, B.A., & Sivakumar, M. (2005). Chemistry of natural products, Narosa publishing house, new delhi, 585.

Liu, Z., Wang, H., Liu, C., Jiang, Y., Yu, G., Mu, X., & Wang, X. (2012). Magnetic cellulose-chitosan hydrogels prepared from ionic liquids as reusable adsorbent for removal of heavy metal ions. *Chem. Commun*., *48*, 7350-7352.

Mansur, H.S., Mansur, A.A., Curti, E., & De Almeida, M.V. (2013). Functionalized-chitosan/quantum dot nano-hybrids for nanomedicine applications: towards biolabeling and biosorbing phosphate metabolites. *J. Mater. Chem. B*, *1*, 1696-1711.

Zhang, Z., Jiang, T., Ma, K., Cai, X., Zhou, Y., & Wang, Y. (2011). Low temperature electrophoretic deposition of porous chitosan/silk fibroin composite coating for titanium biofunctionalization. *J. Mater. Chem*., *21*, 7705-7713.